2011

Flux dynamics in (Y, Nd)1Ba2Cu3O7 superconductors

A S Mahmoud
Al-Fateh University, Libya

Josip Horvat
University of Wollongong, jhorvat@uow.edu.au

S X. Dou
University of Wollongong, shi@uow.edu.au

Eur. Phys. J. Appl. Phys. **53**, 10801 (2011)
DOI: 10.1051/epjap/2010100279

THE EUROPEAN PHYSICAL JOURNAL APPLIED PHYSICS

Regular Article

Flux dynamics in $(Y, Nd)_1Ba_2Cu_3O_{7-\delta}$ superconductors

A.S. Mahmoud[1,a], J. Horvat[2], and S.X. Dou[2]

[1] Department of Physics, Faculty of Science, Al-Fateh University, P.O. Box 13220, Tripoli, Libya
[2] Institute of Superconducting and Electronic Materials, University of Wollongong, NSW 2522 Wollongong, Australia

Received: 14 July 2010 / Accepted: 28 September 2010
Published online: 23 December 2010 –

Abstract. The vortex dynamics of (Y, Nd)$Ba_2Cu_3O_{7-\delta}$ ((Y, Nd)123) superconductors have been studied using magnetic relaxation measurements obtained at different sweep rates. The temperature dependence of the dynamic relaxation rate (Q) is found to be not vanishing at $T = 0$ K, and also showed well developed maxima becoming broader and tending to move to higher temperatures with decreasing magnetic field. At temperatures close to the critical temperature (T_c), $Q(T)$ showed well-developed minima becoming deeper and tending to move to lower temperatures with increasing field. These minima appeared to occur approximately at the same reduced temperature position [T/T_c] as that of oxygen-controlled-melt-grown (OCMG)-Nd(123) samples, thus providing further support for pinning similarities between both systems. Both the field dependence of the characteristic pinning energy [U_c] and relaxation rate showed significant inconsistency with the collective pinning theory but full agreement with the results of [Perkins et al., Phys. Rev. B **54**, 12551 (1996)].

1 Introduction

The static and dynamic disorders are the key elements governing the magnetic vortex matter in high-T_c superconductors [1]. These disorders are responsible for flux-pinning and flux creep phenomena hence their understanding is important for the development of technological applications. Considerable research has been made to theoretically model and practically optimize these vortex effects particularly in the RE(123) materials (RE = rare earth elements) which showed very promising features for industrial applications [1–59].

In our previous work focused on the static disorder in the (Y, Nd)123 system [60], we have shown that scaling of irreversible properties can be described quite well using Dew-Hughes [59], and Perkins and Caplin [30] and Jirsa et al. [27] models. Given the fact that the Perkins and Caplin model [30] has seriously questioned the ability of the collective pinning theory to comprehensively explain the vortex matter phenomena, then our recent results are quite important because they provide support for the Perkins and Caplin model [30]. In this work, we report a study of the vortex dynamics in (Y, Nd)123 superconductors using magnetic relaxation measurements performed at different sweep rates [dynamical approach]. These measurements results in a contradiction with the collective pinning theory, again supporting the Perkins and Caplin model. This paper is organized as follows: first we describe the experimental procedure, and then introduce the theoretical background, followed by discussion of the results and conclusions.

2 Experimental

$(Y_{0.45}, Nd_{0.55})_1Ba_2Cu_3O_{7-\delta}$ samples with the nominal compositions $((Y_{0.5}, Nd_{0.5})_1Ba_2Cu_3O_{7-\delta}$ +20 wt.% $(Y_1, Nd_1)_2Ba_1Cu_1O_{5-\delta}$ +0.5 wt.% $PtO_2)$, and called ((Y, Nd)123) were prepared by melt processing in air, the details of which have been described elsewhere [61]. Identical, rectangular-shaped samples, with typical dimensions $[1.77 \times 1.3 \times 0.95]$ mm^3, were cleaved from a large domain of each melt-processed block. The microstructure of these samples was characterized using an electron probe microanalyzer (EPMA) [60,61]. The samples were twinned and had a $T_c \geqslant 89$ K with a transition width <2 K. The quality of the samples was further checked using magneto-optic imaging and AC-susceptibility techniques.

The dynamical relaxation rate was determined from measurements of magnetic hysteresis loops (MHLs) taken at different sweep rates [1, 3, 5, 10, 15 and 20 mT/s], and over the temperature range 10 K $\leqslant T \leqslant$ 80 K. These measurements were performed using a vibrating sample magnetometer (Oxford instruments) equipped with 12 T magnet, and with the applied field parallel to the c-axis of the sample. At all temperatures, the measurements were proceeded by first cooling the sample in zero field from above the critical temperature, while the field was then applied and ramped, up to sufficiently high fields (typically above the irreversibility field), using all above-mentioned

[a] e-mail: as_mahmoud@hotmail.com

sweep rates. Thus six full, MHLs were produced at each temperature. The current density (J_s), where J_s stands for the current density in the presence of the creep effect ($J_s \leqslant J_c$), was extracted from the measured MHLs using the extended Bean critical-state model expression [62]:

$$J_s = \frac{20\Delta M}{a\left(1 - \frac{a}{3b}\right)},$$

where ΔM is the full width of the magnetization loop in emu/cm^3 during increasing and decreasing field cycles, and a, b ($a \leqslant b$) are the cross-sectional dimensions of the sample perpendicular to the applied field in cm. The value of the critical temperature (T_c) was determined using an AC-susceptometer.

3 Theory

The differential equation governing thermally activated flux creep is expressed as [55]:

$$\frac{\partial \mathbf{B}}{\partial t} = -\nabla x \left[\frac{\mathbf{B} \times (\mathbf{J_s} \times \mathbf{B})}{|\mathbf{B} \times \mathbf{J_s}|} x_0 \omega_0 \exp\left(\frac{-U(j_s, T, B)}{k_B T}\right)\right], \tag{1}$$

where $\mathbf{B}$ is the magnetic induction obtained by averaging the local field inside the superconductor over several penetration depths, $\mathbf{J_s}$ is the supercurrent density, $2x_0$ the hopping distance, and ω_0 the vortex attempt frequency.

For a sample with cylindrical symmetry in a magnetic field B, parallel to the axis of symmetry, equation (1) can be considerably simplified, as $J_s = (0, J_s, 0)$ in cylindrical coordinates (r, ϕ, z). After integration one obtains [17,18]:

$$-\frac{dm}{dt} = \Omega \frac{dJ_s}{dt} = \frac{\chi_0}{\mu_0}\frac{dB}{dt} - \frac{\Delta v_0 B}{\mu_0} \exp\left[-\frac{U(J_s, T, B)}{k_B T}\right], \tag{2}$$

where $\chi_0 = \mu_0\, dm/dB$ is the differential susceptibility, Δ a geometrical factor, Ω the proportionality factor between J_s and the magnetic moment of the sample and $B = \mu_0 H$ is the external applied field. The parameter Ω, χ_0 and Δ depend on the size and shape of the sample. For instance, for a slab shaped sample of thickness $2a$, width b and length c, and with B parallel to the c-direction one has [17]

$$\chi_0 = 2abc, \quad \Delta = bc \text{ and } \Omega = a^2 bc. \tag{3}$$

Equation (2) can be formally solved for $U(J)$:

$$U(J_s) = k_B T \ln\left[\frac{B\Delta v_0}{\mu_0 \frac{dm}{dt} + \chi_0 \frac{dB}{dt}}\right]. \tag{4}$$

It is clear from equation (4) that $U(J_s)$ and consequently J_s depend only on ($\mu_0\, dm/dt + \chi_0\, dB/dt$) and not on the terms dm/dt and dB/dt separately [16,19]. This means that each point of a relaxation curve (where $dB/dt = 0$ by definition) corresponds to an effective sweep rate given by:

$$\left[\frac{dB}{dt}\right]_s = \left[\frac{\mu_0}{\chi_0}\frac{dm}{dt}\right]_R, \tag{5}$$

where S and R denote sweep and relaxation, respectively [16,19]. Equation (5) is valid as long as $\mu_0\, dm/dt \ll \chi_0 dB/dt$, which can be shown to be always the case for sufficiently thin samples such as that used in this study. Therefore, all values of magnetic moment obtained from conventional relaxation measurements can be reproduced by sweeping the magnetic field at an effective sweep rate given by equation (5).

For sweeping rates $\mu_0\, dm/dt \ll \chi_0\, dB/dt$ equation (3) is simplified to:

$$\begin{aligned} U(J_s) &= k_B T \ln\left(\frac{\Delta v_0 B}{\chi_0}\right) - k_B T \ln\left(\frac{dB}{dt}\right) \\ &= k_B T \ln\left(\frac{\Delta v_0 B}{\chi_0 (dB/dt)}\right) = k_B T C, \end{aligned} \tag{6}$$

where C is defined as:

$$C = \ln \frac{2v_0 B}{a(dB/dt)}. \tag{7}$$

By differentiating equation (6) with respect to dB/dt at given values of B and T one obtains

$$\begin{aligned} \frac{dU}{d\ln J_s} &= k_B T \left[\frac{d\ln J_s}{d\ln(dB/dt)}\right]^{-1} \\ &= -k_B T \left[\frac{d\ln m}{d\ln(dB/dt)}\right]^{-1} \end{aligned} \tag{8}$$

i.e.,

$$\frac{dU}{d\ln J_s} = -\frac{k_B T}{Q}, \tag{9}$$

where Q is the dynamical relaxation rate defined as:

$$Q = \frac{d\ln m}{d\ln(dB/dt)} = \frac{d\ln J_s}{d\ln(dB/dt)}. \tag{10}$$

It is clear from the above equations that measurements of Q allow us to straightforwardly determine $dU/d\ln J_s$ and consequently compare with theoretical predications [4]. In references [16,19] it was demonstrated that measurements of Q provide essentially equivalent information about the vortex dynamics as do conventional relaxation measurements, namely, measurements of magnetic moment as a function of time at constant sweep rate. This means that

$$\begin{aligned} Q &= \frac{d\ln m}{d\ln(dB/dt)} = \frac{d\ln j_s}{d\ln(dB/dt)} \\ &= S \equiv R = \frac{d\ln J}{d\ln t} = \frac{d\ln M}{d\ln t}. \end{aligned} \tag{11}$$

Where R is the normalized relaxation rate during conventional relaxation measurements. Further details concerning S and R can be found elsewhere [16].

4 Results and discussion

4.1 Field dependence of Q

Figure 1 shows the field dependence of the magnetic moment measured at different sweep rates [1, 3, 5, 10, 15

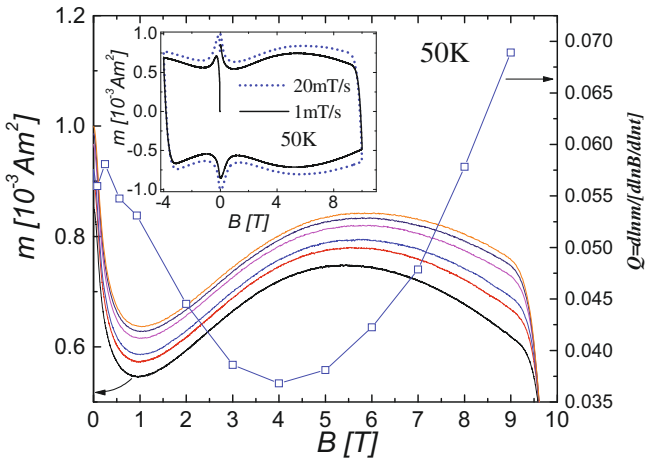

Fig. 1. (Color online) Field dependence of the magnetic moment and dynamical relaxation rate at $T = 50$ K for the (Y, Nd)123 melt-processed sample. The magnetic field was applied parallel to the c-axis of the sample and swept with a rate of [from top to bottom: 20, 15, 10, 5, 3 and 1 mT/s]. Inset: full magnetic hysteresis loops at the same temperature with different sweeping rates.

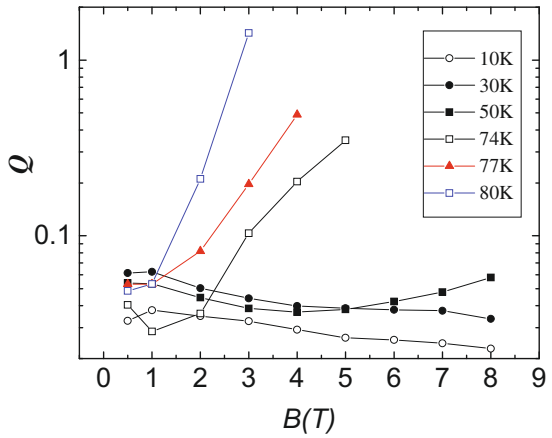

Fig. 2. (Color online) Semi-log plots for the field dependence of the normalized dynamical relaxation rate $Q(B)$ at different temperature for the (Y, Nd)123 melt-processed sample. The figure emphasizes the correlation between the $m(B)$ shape and the $Q(B)$ plot as indicated by the presence of minimum in $Q(B)$ at temperatures where the fishtail peak effect can be seen.

and 20 mT/s] and the corresponding dynamical relaxation rate, Q, for the (Y, Nd)123 melt-processed sample at $T = 50$ K. The magnetic field was applied parallel to the c-axis of the sample. Typical plots of full m-B loops corresponding to 1 and 20 mT/s are shown in the inset. Q was determined from the measured $m(B)$ data using equation (10). From Figure 1 it is clear that for all fields the increase of sweeping rate leads to an increased magnetization and shifts the fishtail peak effect and irreversibility fields towards larger values. This shift of the peak field value with sweep time to lower values was highlighted in reference [34] to indicate that the fish-tail peak field [B_{jp}] cannot represent a phase transition line but is rather likely a crossover in the dynamics from elastic to plastic flux creep. Proving such a crossover for a melt-processed sample is almost impossible due to the large number of defects. Furthermore, it is clear from Figure 1 that the relaxation is rather significant at fields larger than the fishtail peak effect than at smaller fields. This suggests a close relationship between the $m(B)$ loop and the relaxation process. To emphasize this point, we present in Figure 2 the $Q(B)$ at all temperatures including $T = 50$ K. From both Figures 1 and 2 we can see the presence of a decreasing and then an increasing behavior, separated by the temperature-dependent minimum for temperatures where the peak effect can be seen, and the absence of this minimum and the presence of only increasing $Q(B)$ behavior over the whole superconducting state for temperatures where no fishtail peak effect was observed. These features clearly confirm the presence of a correlation between the $m(B)$ shape and the relaxation process. For all data, it is clear that the relaxation process is strongly influenced by temperature. This effect is marked by almost a decreasing behavior at low temperatures, plateau-like shape at medium temperatures and a rapid increase of $Q(B)$ to a maximum value at high temperatures. For the low temperature data, up to the maximum field available, no upturn or a minimum in the $Q(B)$ behavior was noticed. However, from the general trend, one would expect that for each of these temperatures a minimum at larger fields would be seen.

The correlation between $Q(B)$ and $m(B)$ in terms of shape has been highlighted in several studies [13,27–30,34–42]. In reference [35], the authors have reported a mirror image like behavior between both parameters, and based on this they have ascribed the fishtail peak effect to a pinning crossover from a single vortex into a bundle vortex regime. However, such a mechanism was soon disputed by a number of studies which in contrast revealed no mirror image correlation between $m(B)$ and the relaxation rate at higher temperatures [13,27–30,36–42]. Such a mechanism is certainly not consistent with our results as they do not show a mirror image between both parameters (see Fig. 1).

4.2 Temperature dependence of Q

Figure 3 shows the temperature dependence of Q for magnetic fields of 0.5, 1, 2, 3, 4, 5 and 6 T applied parallel to the c-axis of the sample. It is clear from Figure 3 that extrapolating the low temperature data down to $T = 0$ shows that Q does not vanish, as expected from the thermally activated flux creep models, rather it exhibits a finite value at that temperature. This behavior is ascribed to the so-called quantum tunneling of vortices taking place at low temperatures and is well documented in references [20–22,24,31,32,43–49]. Similar to normal flux creep, quantum creep of vortices can also be a thermally assisted process. In fact, pure "quantum vortex creep" is believed to take place only at ultra low temperatures, typically below 1 K [24]. In the work of Wen et al. [24] on Y(123) and Y(124) films, the appreciable effect of thermally assisted quantum creep was confined to below ∼(10–13) K,

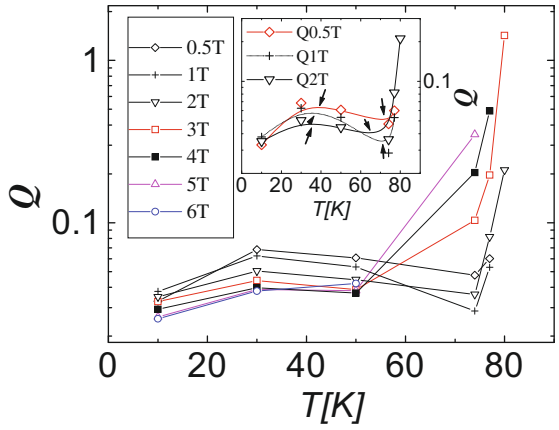

Fig. 3. (Color online) Semi-log plots for the temperature dependence of the normalized dynamical relaxation rate $Q(T)$ under different magnetic fields. The figure shows minima and maxima taking place at relatively low and high temperatures, respectively. Note also that Q does not vanish at $T = 0$ K, which is due to a quantum creep effect. Inset, better insight emphasizing the change of characteristics of $Q(T)$ maxima and minima as a function of field. Lines are guides to the eye.

while for BSCCO a lower temperature (e.g. $T \sim 5$ K) was assigned by van Dalen et al. [21]. These differences in the quantification of quantum vortex creep between both materials, may be understood within the difference in the superconducting nature of both materials particularly as regards anisotropy. In our case, as no measurements were performed below 10 K, no attempt was made to estimate analogous temperatures. However, as our analysis of the vortex dynamics are based on the thermally assisted flux creep model, therefore missing such an estimation is certainly not significant.

In the temperature range from $T = 10$ K to $T \sim 70$ K, it is obvious that the $Q(T)$ data shows three characteristic features: the presence of pronounced maxima at $T < 0.5T_c$, the presence of minima at $T > 0.5T_c$ and the rapid increase of Q which become steeper with increasing field and upon approaching T_c. In the later region [upon approaching T_c] it is important noting that, the uncertainty in determining the irreversible magnetization ($M_{\rm irr}$) becomes quite considerable due to technical limitations, therefore determining the true behavior of $Q(T)$ becomes very difficult.

While, for most cases, determining the precise positions of $Q(T)$ maxima and minima is a difficult task due to insufficient data points particularly at low temperatures, we can easily prove that the maximum of $Q(T)$ (*apparently at* $T \sim 30$ K) exhibits a smaller height, becomes less broad and tends to move towards lower temperatures with increasing magnetic field strength. Furthermore, the minimum of $Q(T)$ shifts towards lower temperatures with increasing magnetic field. These observations are similar to published data [19,21,24,25] thus providing further support for our conclusions. For various reasons, comparison of our data with those of Y(123) and Nd(123) systems is specifically important as it can provide valuable information regarding the pinning characteristics of these systems. From such a comparison, we learn that while most RE(123) samples (including(Y, Nd)123 system) [25,49] exhibit similar $Q(B)$ characteristics, in terms of $Q(T)$ they show some important differences. For OCMG-Nd(123) [25] and our (Y, Nd)123 system one can note that under 1 T applied fields, both systems appeared to exhibit a Q maximum at almost the same temperature, ∼30 K, which is different from $T = 20$ K commonly reported for Y(123) at the same field [33]. More importantly, for both (Y, Nd)123 and OCMG-Nd(123) systems, the position of the minimum in the $Q(T)$ data is located at higher temperatures than that of Y(123). In fact, if we take the T_c of a material into consideration, then it is easy to prove that both the $Q(T)$ minima of OCMG-Nd(123) $[(T_{\rm min}/T_c) = 80/93.4 = 0.84)]$ and (Y, Nd)123 $[(T_{\rm min}/T_c) \sim 77/89 = 0.83]$ occur at the same position, which is again larger than the $[(T_{\rm min}/T_c) = 60/93 = \sim 0.65]$ that one obtains for Y(123) [50]. These results suggest remarkable similarity in pinning properties between Nd-based systems which is in full agreement with our scaling results described elsewhere [60]. Note that the presence of $Q(T)$ minimum seems to be a general characteristic for all RE(123) systems including the Pr-doped Y(123) system [52], however, the position of such a minimum at high temperature reflect good pinning properties in the sample [25]. In this regard, any pinning mechanism active at high temperatures, such as spatial variation of T_c due to RE^1/RE^2 and/or RE/Ba exchange effects [53] or analogously oxygen deficient regions [54] can give rise to such a $Q(T)$ minimum.

4.3 Consistency of experimental results with the collective pinning theories

To analyze the vortex dynamic properties in a superconductor there are several models proposed in the literature. The collective pinning (CP) [4] and vortex glass (VG) [10] theories are widely used in the literature. For both theories the current dependence of the activation energy $U(J_s)$ is predicated to obey an interpolation formula [4,10]:

$$U(J_s) = \frac{U_c}{\mu}\left[\left(\frac{J_c}{J_s}\right)^{\mu} - 1\right], \qquad (12)$$

where U_c is the characteristic pinning energy and μ is a parameter which depends on the pinning characteristics. The significance of this formula is that it contains all other forms proposed so far for $U(J_s)$. The Anderson-Kim model [51], for example, is obtained when $\mu = -1$ while that of Zeldov et al. [11,12] corresponds to $\mu = 0$.

In its simplest version, the VG model predicts μ to be a universal exponent less than 1, while the CP theory predicted a complicated dependence of μ on the dimensionality and the particular flux creep regime, which in turn depends on field and temperature. In the case of three dimensional (3D) pinning, the Feigel'man et al. version predicts $\mu = 1/7$, 3/2 and 7/9 for pinning of a single vortex (SV), small flux bundles (SB) and large flux bundles (LB), respectively. For two dimensional (2D) creep

$\mu = 9/8$ and $\mu = 1/2$ are proposed for a single vortex and collective vortex creeps, respectively. More recently it was shown that in the case of collective vortex creep a differentiation of small, medium and large bundle pinning leads to $\mu = 7/4$, 13/16, 1/2 [56].

To explore the pinning behavior in a superconductor, in terms of the CP and VG theories, several parameters can be usefully used. Among them μ, J_c and U_c are directly relevant. However, μ is the most significant one. Various methods can be used to determine this parameter [16,24,26], but it depends on the type of measurement and on the specific purpose as to which technique is preferred. For dynamically measured magnetic relaxation data, there are at least two techniques by which μ can be determined [16,26]. These techniques can also determine U_c and J_c which are quite significant. In the following, we use these techniques to determine both these parameters and also to examine their significance as far as characterization of the flux creep properties of a superconductor are concerned, particularly in relation to the CP theory.

In reference [24] it was shown that plotting T/Q versus T leads straightforwardly to U_c and, if C is known, to μ. This can be understood by the following: inserting equation (12) into equation (9) one obtains

$$J_s = \frac{J_c}{\left[1 + \frac{\mu k_B T}{U_c} \ln\left(\frac{2v_0 B}{adB/dt}\right)\right]^{1/\mu}}. \tag{13}$$

For the dynamical relaxation rate, Q, defined in equation (6) and if μ is independent of the current, it follows that:

$$Q = \frac{1}{\frac{U_c}{k_B T} + \mu \ln\left(\frac{2v_0 B}{adB/dt}\right)} \tag{14}$$

which together with equation (7) leads to:

$$\frac{T}{Q} = \frac{U_c}{k_B} + \mu C T. \tag{15}$$

Here it is clear that a plot of T/Q versus T will lead to a straight line with a slope equivalent to μC and intercept of U_c/k_B. Clearly, to determine μ, C must be determined. In principle, this can also be made directly or indirectly from the experimental data. Alternatively, for some materials one may depend on the literature to guess a starting value for such a parameter. For the RE(123) system, for example, C is commonly reported to be between 14 and 20 [29,30].

In Figure 4 we show plots of T/Q versus T at different magnetic fields for the studied sample. The data shows almost similar behavior to the $Q(T)$ data. However, the deviations at high temperatures can now be better understood in terms of the temperature dependence of U_c and thermal fluctuations close to the irreversibility line. By extrapolating the data down to $T = 0$ K, U_c is determined. By repeating the same procedure for the other magnetic field data, the field dependence of U_c is determined. The results are shown in Figure 5. It is clear that U_c shows a decreasing, power-law dependence with increasing B up

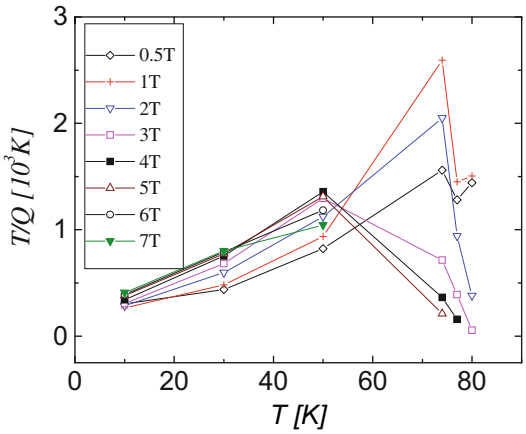

Fig. 4. (Color online) Temperature dependence of the ratio T/Q for the (Y, Nd)123 melt-processed sample. According to equation (15), proper extrapolation for the low temperature data down to zero determines both μC (the slop) and U_c [K] (the intercept).

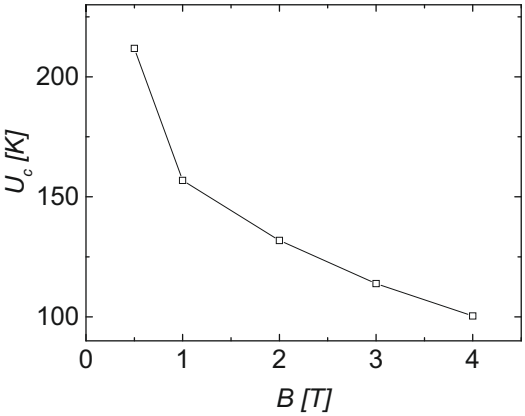

Fig. 5. Magnetic field dependence of U_c [K] for the (Y, Nd)123 melt-processed sample as determined from the zero-temperature intercept of the T/Q versus T data. Note that U_c shows a decreasing behavior with field, which is in stark contrast with the predications of the CP theory.

to $B = 4$ T, which is in stark contrast with the results of van Dalen et al. [22] where U_c was reported to increase with B. However, our results are consistent with the model developed recently by Perkins et al. [29] and Perkins and Caplin [30] where the field dependence of U_c was predicated to obey a power-law form, $U_c \propto B^{-\alpha}$ and where $\alpha \sim 1$ was found experimentally. In our case best fitting of the data resulted in $\alpha = 0.3$, which is markedly different from $\alpha \sim 1$ reported in reference [29]. Such a difference may be ascribed to: first U_c is already assumed to be independent of temperature in our case, whereas it is treated as a temperature-dependent parameter in references [29,30]. Here, it is important to indicate that our assumption was based on the fact that in all existing theories U_c is found to vary only weakly with temperature [58]. Second, the result $\alpha \sim 1$ was found for a single crystal sample which should differ from that of a melt-processed sample where a larger number of stronger pinning center (e.g. RE(211) inclusions) exist. Furthermore, at low

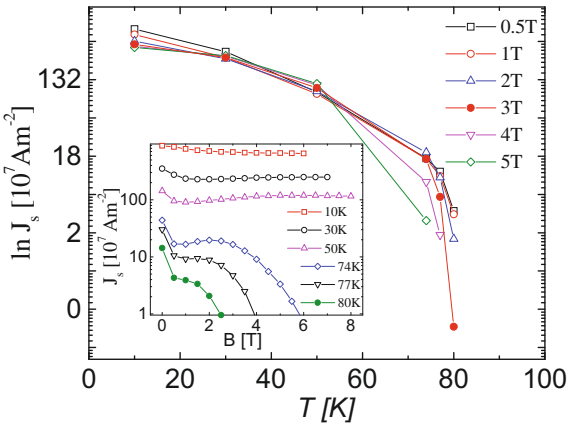

Fig. 6. (Color online) Plots of temperature dependence of $(\ln J_s)$ for the (Y, Nd)123 melt-processed sample. Inset, field dependence of J_s as determined from measurements of magnetic hysteresis loops with sweeping rate of 1 mT/s.

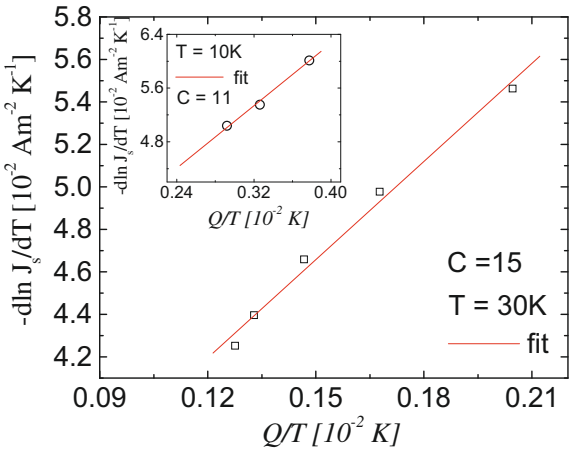

Fig. 7. (Color online) Plots of $-d\ln J_s/dT$ versus Q/T at $T = 30$ K and $T = 10$ K (inset) for different magnetic fields. From the slop of the linear fit to the data we obtain $C = 11$ and 15 at $T = 10$ K and $T = 30$ K, respectively.

temperatures our data is sparse and this can result in a larger uncertainty in determining U_c and hence α.

Having determined U_c we now determine C in order to determine μ. For magnetic relaxation data obtained based on a dynamical approach, the only technique, to the best of our knowledge, that can be used to determine the $U(J_s)$ dependence is the generalized inversion scheme developed by Schnack et al. [18]. An advantage of this technique is that it includes all other techniques as special cases. In reference [24] the following equation was derived:

$$-\frac{d\ln J_s}{dT} = -\frac{d\ln J_C}{dT} + C\frac{Q}{T}. \qquad (16)$$

According to Wen et al. [24], this formula is valid for temperatures where the quantum creep can be ignored at low temperatures. The corresponding region is different from sample to sample. Close inspection of the data shows that determining C within the temperature range $10\ \text{K} \leqslant T \leqslant 30\ \text{K}$ appears to be reasonable. However, we found it more useful to determine C at both $T = 10$ K and $T = 30$ K and then determine the average value rather than determine it at a temperature lying in the middle between $T = 10$ K and $T = 30$ K. This will tell us more about whether or not assuming C independent of temperature is reasonable. Since $J_c(B,T)$ can be expressed as a product of field and temperature dependent functions (Ref. [18]), the component $d\ln J_c/dT$ is independent of magnetic field. Thus, a plot of $d\ln J_s/dT$ versus Q/T should lead to a straight-line with a slope equivalent to C.

In Figure 6 we show the temperature and field dependencies of the measured current density ($J_s(B)$ at $T = 10$, 30, 50, 74, 77 and 80 K. The data was determined from the magnetic hysteresis loops measured using the 12 T VSM, with J_s being calculated using the Bean model [62]. Note, however, that J_s obtained here is different from that obtained based on SQUID measurements, which can be justified by the difference in the way they measure the magnetic moment of a sample. Using Figures 4 and 6 to determine $d\ln J_s/dT$ and the corresponding Q/T, Figure 7 shows typically $d\ln J_s/dT$ as a function of Q/T at $T = 10$ K and 30 K for different magnetic fields. It is clear from this figure that the data falls remarkably onto a straight line with slope $C = 11$ at $T = 10$ K and $C = 15$ at $T = 30$ K. Thus an averaged $C \sim 13$ is obtained. This value is very close to the range of values [14–20] commonly reported for C in the literature [22,24,57]. It is already evident that the determination of μ using this method will end up as an averaged value as the parameter C is an averaged value. It must be noted that assuming C as a constant over the entire range of temperatures and fields is not strictly valid, and could result in false conclusions as far as the analysis of pinning is concerned. Thus, it is meaningless to determine μ using this approach. We will determine this parameter using an alternative technique to be presented after the calculations of the true critical current density, J_c.

To calculate the true critical current density, Schnack et al. [18] have developed the so-called generalized inversion scheme (GIS). This approach is centered on the hypothesis that the current and temperature dependencies of the activation energy of a superconductor can be separated into a product of temperature and field dependent functions as follows:

$$U(J_s, T, B) = g(T, B)f(J_s/J_c(T, B)). \qquad (17)$$

This model assumes that U_c and J_c are dependent on each other according to a power-law form, that is,

$$g(T, B) \propto U_c(T, B) \propto [J_c(T, B)]^p G(T), \qquad (18)$$

where J_s and J_c are the measured and the true critical current densities; U_c is the characteristic pinning energy; $G(t) = (1 + t^2)^l(1 - t^2)^m$ is a thermal function with l, m and p parameters dependent upon the dimensionality of the superconductor under investigation and on the vortex creep regime through the parameter, $t = T/T_c$.

For instance, for a collectively pinned single vortex in three dimensions (3D) the pinning energy is given by $U_c = J_c\phi_0 L_c\xi$ where ϕ_0 is the flux quantum ξ is the coherence length and $L_c \propto J_c^{-1/2}$ is the correlation length,

which is restricted by the thickness of the layer and hence is independent of the current density [18]. Hence $p = 1/2$ and $p = 1$ are obtained for a collectively pinned single vortex in 3D and 2D, respectively. Analogously, for other pinning regimes and vortex dimensionalities different values for p have been derived. For example, for small vortex bundle pinning $p = -3/2$ and $p = -1/2$ for 3D and 2D cases, respectively, while $p = -1/2$ and $p = 0$ were derived for large vortex bundle pinning in the 3D and 2D cases, respectively [24]. As m and l are similar to the p dependence on the dimensionality and the pinning regimes, then analogously different values of l and m have been reported to correspond to different p values. In short, these values are summarized as follows: for 3D (SV, $(l,\ m) = (5/4, -1/4)$, SB, $(l,\ m) = (17/4, 3/4)$, LB, $(l,\ m) = (7/4, -3/4)$), while for 2D (SV, $(l,\ m) = (1/2, -1/2)$, SB, $(l,\ m) = (11/4, 1/4)$, LB, $(l,\ m) = (3/2,\ -1/2)$).

With the development of the GIS approach one may derive the following formula for calculating the true critical current density of a superconductor at any temperatures under the same field [18]:

$$J_c(T_i) = J_c(T_i) \exp \left\{ \int_{\ln T_i}^{\ln T_{i+1}} \frac{CQ\left(1 - \frac{d\ln G}{d\ln T}\right) d\ln T}{1 + pCQ} + \int_{\ln J_s(T_i)}^{\ln J_s(T_{i+1})} \frac{d\ln j_s}{1 + pCQ} \right\}, \quad (19)$$

where C is a constant defined by equation (7) and Q is the dynamical relaxation rate. In principle, except for p, all parameters on the right hand side can be accessed directly or indirectly from experiment. To begin the calculation using this procedure, one first needs to determine $J_c(T_0)$, that is, the critical current density at the lowest temperature at which the current density was measured. In turn, this requires the determination of $J_c(0)$, that is, the critical current density at $T = 0$ K. As the whole GIS is based on the principle of thermally activated vortex motion, the low temperature data including $J_c(0)$ must be corrected properly from the quantum creep effect. Since J_s decreases exponentially with increasing temperature except at low temperatures, then the proper extrapolation to the linear part of the T-dependent ($\ln J_s$) data will lead to $J_s(0)$, the current density that should appear at $T = 0$ K if no quantum creep is present in the sample [22]. As the thermal activation of vortices should vanish at $T = 0$ K, then $J_s(0)$ is in fact, the true critical current density, $J_c(0)$. In Figure 8 we show the field dependence of $J_c(0)$ for our (Y, Nd)123 sample.

Having obtained $J_c(0)$, we can now determine $J_c(T_0)$ according to the procedure outlined in references [24,57] and then, using equation (19), the true critical current density $J_c(T)$ of the sample at different temperatures. The results obtained are shown in the inset to Figure 8, which shows at $B = 0.5$ T, the temperature dependence of the *true* critical current density. For comparison, the temperature dependence of the measured current density J_s is also shown. In these J_c calculations only $p = 0.5$ was able

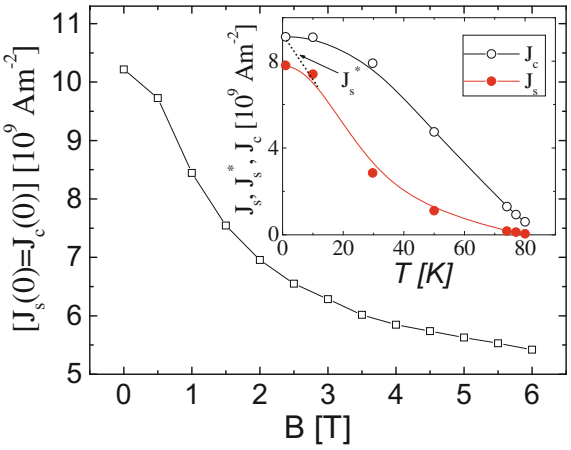

Fig. 8. (Color online) Field dependence of the zero-temperature current density, $J_s(0) = J_c(0)$, obtained from the extrapolation of $\ln J_s$ versus T data to $T = 0$ K [24]. Inset: temperature dependence of the true critical current density as calculated by means of the GIS for the (Y, Nd)123 melt-processed sample with $B = 0.5$ and $p = 0.5$. The measured current density is shown for comparison. The dashed line corresponds to $J_s^*(T)$, the current density in the absence of quantum creep.

to yield a physically meaningful result. For the other p values, the data was found to either diverge or converge ($J_c < J_s$) at certain temperatures ($T < T_c$), which are not accepted physically.

Despite the number of attempts we have made to extend this procedure to the other magnetic fields, physically acceptable solutions could not be obtained. Part of this problem may be due to the sparseness of our data, which makes the calculations at larger fields rather difficult. Such a major disadvantage has made it difficult to compare between the Griessen et al. [58] and Dew-Hughes [59] models, in terms of characterizing the dominant pinning mechanism in a superconductor. This comparison is important in order to understand whether or not both models can lead to the same physics.

To determine μ from magnetic relaxation data, the simplest way is to use the method of Jirsa et al. [16], that is, from a plot of $[d\ln m/d\ln(dBe/dt)]^{-1}$ as a function of $\ln(dB/dt)$. μ is then just the slope of the data, which is assumed to show a straight-line behavior. The theoretical basis of this procedure is derived as follows. From equation (12) one obtains:

$$\frac{dU}{d\ln J_s} = \mu U(J_s) - U_C. \quad (20)$$

Combining equation (13) with equations (6) and (8) leads to:

$$\left[\frac{d\ln m}{d\ln(dB/dt)}\right]^{-1} \left[\frac{d\ln m}{d\ln(dB/dt)}\right]^{-1} = -\ln\left(\frac{dB}{dt}\right) + \mu n \left(\frac{\Delta v_0 B}{\chi_0}\right) - \frac{U_c}{k_B T}. \quad (21)$$

Equation (21) suggests that μ determined in this way would be a single value at each temperature data point

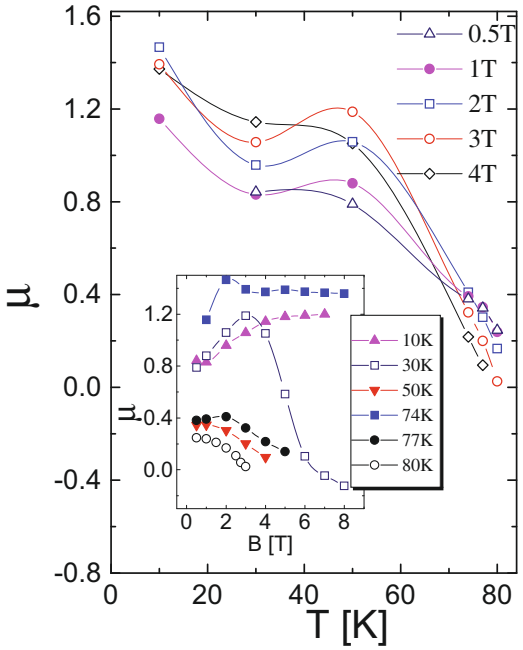

Fig. 9. (Color online) Temperature and field (inset) dependencies of μ as determined using equation (21). Lines are guides to the eye.

and not averaged over a number of temperatures as is often found through the $U(J)$-fitting method. To determine μ using equation (21), clearly one has to plot, in semi-log format, $1/Q$ versus sweeping rate. By doing this we have found that all data collapses into a straight line whose slope determines μ. By applying the same procedure at different fields and over all temperatures, the field and temperature dependencies of μ have been determined. The temperature and field dependencies of μ are shown in Figure 9. It is clear from these figures that the data is hardly consistent with the predications of the CP theory. Part of this disagreement may be ascribed to the uncertainty in determining μ, but such an effect cannot be so dominant as to produce such a significant discrepancy. Such behavior can seriously question either the procedure of Jirsa et al. [16] or the comprehensiveness of the CP theory as being considered as the single model that can fully explain the complete vortex properties in high-T_c superconductors.

A closer look at the literature shows that, in most cases the CP theory has failed to show it self as a general model to solve the flux pinning problems in high-T_c superconductors. This is particularly clear from the inability of the theory to fit most of the experimental data. In fact, in many cases major discrepancies between the CP theory and experimental results can be found. For example, for all the CP regimes, S is predicated to either decrease or remain constant with increasing magnetic field [29,30]. This is in contrast with experimental data, including ours, where in fact S increases with increasing field. In addition, the CP predicates U_c to increase with B, because of a stiffening of the vortex lattice as it becomes denser leading to larger correlated bundles. In fact, one finds for most experimental data, just the opposite [29,30]. In addition, the CP theory assumes current densities much lower than the critical current density, a case which is dependent largely on the sweep rate used during the experiment. Data measured at a high sweep rate is clearly not suitable to be modeled according to the CP theory.

5 Conclusion

The vortex dynamics of (Y, Nd)123 superconductors were studied using magnetic relaxation measurements undertaken at different sweep rates. The fishtail peak effect and the irreversibility fields were found to be decreased with increasing sweep rate (decreasing time), suggesting the importance of vortex dynamics for the formation of the fishtail peak effect. However, a mirror image correlation between the field dependence of $m(B)$ and that of the relaxation rate $Q(B)$ was not found. The temperature dependence of Q indicated a crossover from the quantum creep regime taking place at low temperatures into thermally activated flux creep which was dominant at higher temperatures. This argument is based on the non-vanishing of Q at $T = 0$ K, and also on the presence of well developed maxima becoming broader and tending to move to higher temperatures with decreasing magnetic field. At high temperatures, $Q(T)$ showed well-developed minima becoming deeper and tending to move to lower temperatures with increasing field. We have shown that these characteristics are similar to those found for OCMG-Nd(123) samples, reflecting similar pinning properties between both materials, which is in full agreement with the scaling results. Attempts to characterize pinning within the framework of the collective pinning theories have failed due to the remarkable inconsistency found between our data and the predications of the collective pinning theory. This was particularly clear in the increasing and decreasing behaviors of S and U_c, respectively, with increasing field, where both are in sharp contrast with the predications of the collective pinning theory.

A. Mahmoud is grateful to F. Klaassen (Faculty of Physics and Astronomy, Vrije University, Netherlands) and M. Jirsa (Institute of Physics, Academy of Sciences of the Czech Republic) for valuable comments.

References

1. G. Blatter, M.V. Feigel'man, V.B. Geshkenben, A.I. Larkin, V.M. Vinokur, Rev. Mod. Phys. **66**, 4 (1994)
2. Y. Yeshurun, A.P. Malozemoff, A. Shaulov, Rev. Mod. Phys. **68**, 911 (1996)
3. M.P.A. Fisher, Phys. Rev. Lett. **62**, 1415 (1989)
4. M.V. Feigel'man, V.B. Geshkenbein, A.I. Larkin, V.M. Vinokur, Phys. Rev. Lett. **63**, 2303 (1989)
5. M.V. Feigel'man, V.B. Geshkenbein, V.M. Vinokur, Phys. Rev. B **43**, 6263 (1991)
6. M.V. Feigel'man, V.M. Vinokur, Phys. Rev. Lett. **41**, 8986 (1990)

7. C.W. Hagen, M.R. Bom, R. Griessen, Phys. Rev. Lett. **62**, 2857 (1989)
8. C.W. Hagen, R. Griessen, in *Studies of high temperature superconductors: advances in research and applications*, Vol. 3, edited by A.V. Narlikar (Nova Science, New York), p. 159
9. C.W. Hagen, R. Griessen, E. Saomons, Physica C **157**, 199 (1989)
10. P. Malozemoff, M.P.A. Fisher, Phys. Rev. B **42**, 6784 (1990)
11. E. Zeldov, N.M. Amer, G. Koren, A. Gupta, R.J. Gambino, M.W. McElfresh, Phys. Rev. Lett. **62**, 3093 (1989)
12. E. Zeldov, N.M. Amer, G. Koren, A. Gupta, M.W. McElfresh, R.J. Gambino, Appl. Phys. Lett. **56**, 680 (1990)
13. Y. Yeshurun, E.R. Yacoby, L. Klein, L. Burlachkov, R. Prozorov, N. Bontemps, H. Wühl, V. Vinokur, in *Proc. of the 7th Int. Workshop on Critical Currents in Superconductors, Alpbach, Austria, 1994*, edited by H.W. Weber (World Scientific, Singapore, 1994), p. 237
14. L. Půst, Supercond. Sci. Technol. **39**, 598 (1990)
15. L. Půst, J. Kadlecova, M. Jirsa, S. Durcok, J. Low Temp. **78**, 179 (1990)
16. M. Jirsa, L. Půst, H.G. Schnack, R. Griessen, Physica C **207**, 85 (1993)
17. H.G. Schnack, R. Griessen, J.G. Lensink, C.J. van der Beek, P.H. Kes, Physica C **197**, 337 (1992)
18. H.G. Schnack, R. Griessen, J.G. Lensink, Hai-Hu Wen, Phys. Rev. B **48**, 13178 (1993)
19. J.J. van Dalen, M.R. Koblischka, R. Griessen, Physica C **259**, 157 (1996)
20. A.J.J. van Dalen, R. Griessen, S. Libbrecht, Y. Bruynseraede, E. Osquiguil, Phys. Rev. B **54**, 1366 (1996)
21. A.J.J. van Dalen, R. Griessen, M.R. Koblischka, Physica C **257**, 271 (1996)
22. A.J.J. van Dalen et al., Physica C **250**, 265 (1995)
23. H.H. Wen, Z.X. Zhao, R.J. Wijngaarden, J. Rector, B. Dam, R. Griessen, Phys. Rev. B **52**, 4583 (1995)
24. H. Wen, H.G. Schnack, R. Gressen, B. Dam, J. Rector, Physica C **241**, 353 (1995)
25. J.J. van Dalen, M.R. Koblischka, H. Kojo, K. Sawada, T. Higuchi, M. Murakami, Supercond. Sci. Technol. **9**, 659 (1996)
26. M. Reissner, J. Lorenz, Phys. Rev. B **56**, 6273 (1997)
27. M. Jirsa, L. Půst, D. Dlouhý, M.R. Koblischka, Phys. Rev. B **55**, 3276 (1997)
28. A. Zhukov, H. Küpfer, G. Perkins, L.F. Cohen, A.D. Caplin, S.A. Klestov, H. Claus, V.I. Voronkova, T. Wolf, H Wühl, Phys. Rev. B **51**, 12704 (1995)
29. G.K. Perkins, L.F. Cohen, A.A. Zhukov, A.D. Caplin, Phys. Rev. B **51**, 8513 (1995)
30. G.K. Perkins, D. Caplin, Phys. Rev. B **54**, 12551 (1996)
31. A. Hamzic, L. Fruchter, I.A. Campbell, Nature (London) **345**, 515 (1990)
32. L. Fruchter, A.P. Malozemoff, I.A. Campbell, J. Sanchez, M. Konczykowski, R. Griessen, F. Holtzberg, Phys. Rev. B **43**, 8709 (1991)
33. L. Civale, A.D. Marwick, W.M. McElfresh, T.K. Worthington, A.P. Malozemoff, F.H. Holtzberg, J.R. Thompson, M.A. Kirk, Phys. Rev. Lett. **65**, 1164 (1990)
34. Y. Abulafia, A. Shaulov, Y. Wolfus, R. Prozorov, L. Burlachkov, Y. Yeshurun, D. Majer, E. Zeldov, H. Wühl, V.B. Geshkenbein, V.M. Vinokur, Phys. Rev. Lett. **77**, 1596 (1996)
35. L. Krusin-Elbaum, L. Civale, V.M. Vinokur, F. Holtzberg, Phys. Rev. Lett. **69**, 2280 (1992)
36. H. Kupfer, S.N. Gordeev, W. Jahn, R. Kresse, R. Meier-Hirmer, Th. Wolf, A.A. Zhukov, K. Salama, D. Lee, Phys. Rev. B **50**, 7016 (1994)
37. S.N. Gordeef, W. Jahn, A.A. Zhukov, H. Kupfer, Th. Wolf, Phys. Rev. B **49**, 15420 (1994)
38. H. Küpfer, Th. Wolf, C. Lessing, A.A. Zhukov, X. Lancon, R. Meier-Hirmer, W. Schauer, H. Wühl, Phys. Rev. B **58**, 2886 (1998)
39. M. Jirsa, A.J.J. van Dalen, M.R. Koblischka, G. Ravi Kumar, R. Griessen, in *Proc. of the 7th Int. Workshop on Critical currents in Superconductors, Alpbach, Austria, 1994*, edited by H.W. Weber (World Scientific, Singapore, 1994), p. 221
40. A.A. Zhukov, L.F. Cohen, G.K. Perkins, A.D. Caplin, S.A. Klestov, V.I. Voronkova, A. Marshall, S. Abell, Physica B **194**, 1921 (1994)
41. L.F. Cohen, A.A. Zhukov, G.K. Perkins, H.J. Jensen, S.A. Klestov, V. Voronkova, S. Abell, H. Küpfer, Th. Wolf, A.D. Caplin, Physica C **230**, 1 (1994)
42. H. Küpfer, S.N. Gordeev, W. Jahn, R. Kresse, R. Meier-Hirmer, Th. Wolf, A.A. Zhukov, K. Salama, D. Lee, Phys. Rev. B **43**, 130 (1991)
43. A.C. Mota, A. Pollini, P. Visani, K.A. Muller, J.G. Bednorz, Phys. Scr. **37**, 823 (1988)
44. A.C. Mota, G. Juri, A. Pollini, T. Teruzzi, K. Aupke, B. Hilti, Physica C **185-189**, 343 (1991)
45. P. Aupke, T. Teruzzi, P. Visani, A. Amann, A.C. Mota, V.N. Zavaritsky, Physica C **209**, 255 (1993)
46. L. Fruchter, A.P. Malozemoff, I.A. Campbell, J. Sanchez, M. Konczykowski, R. Griessen, F. Holtzberg, Phys. Rev. B **43**, 8709 (1991)
47. J. Tejada, E.M. Chudnovsky, A. Garcia, Phys. Rev. B **47**, 11552 (1993)
48. G.T. Seidler, C.S. Carillo, T.F. Rosenbaum, U. Welp, G.W. Carbtree, V.M. Vinokur, Phys. Rev. Lett. **70**, 2814 (1993)
49. G.T. Seidler, T.F. Rosenbaum, K.A. Beauchamp, H.M. Jaeger, G.W. Carbtree, U. Welp, V.M. Vinokur, Phys. Rev. Lett. **74**, 1442 (1995)
50. P.J. Kung, M.P. Maley, M.E. Mchenery, J.O. Willis, M. Murakami, S. Tanaka, Phys. Rev. B **48**, 13922 (1993)
51. P.W. Anderson, Y.B. Kim, Rev. Mod. Phys. **36**, 39 (1964)
52. Y.G. Xiao, B. Lin, J.W. Li, Z.X. Zhao, H.T. Ren, L. Xiao, X.K. Fu, J.A. Xia, Supercond. Sci. Technol. **7**, 623 (1994)
53. M. Murakami, S.I. Yoo, T. Higuchi, N. Sakai, J. Weltz, N. Koshizuka, S. Tanaka, Jpn J. Appl. Phys. **33**, L715 (1994)
54. M. Däumling, J.M. Seuntjens, D.C. Larbalestier, Nature **346**, 332 (1990)
55. E.H. Brandt, Supercond. Sci. Technol. **5**, 25 (1992)
56. V.M. Vinokur, P.H. Kes, A.E. Koshelev, Physica C **248**, 179 (1995)
57. F. Klaassen (private communication)
58. R. Griessen, H.H. Wen, A.J.J. van Dalen, B. Dam, J. Rector, Physica C **241**, 353 (1995)
59. D. Dew-Hughes, Philos. Mag. **30**, 293 (1974)
60. A.S. Mahmoud, G.J. Russell, M.R. Koblischka, N. Chickomoto, M. Murakami, Physica C **415**, 40 (2004)
61. A.S. Mahmoud, G.J. Russell, Physica C **322**, 193 (1999)
62. C.P. Bean, Phys. Rev. Lett. **8**, 250 (1962)